Equation of state for core collapse supernova simulation and neutron star core

Sarmistha Banik*
Saha Institute of Nuclear Physics, APC Division, Kolkata, INDIA

A phase transition from hadronic to exotic phases might occur in the early post-bounce phase of a core collapse supernova. We investigate the role of strange baryons in the dynamical collapse of a non-rotating massive star to a black hole using 1D General relativistic simulation *GR1D*. We choose a $40M_{solar}$ progenitor of Woosely and follow the dynamical formation of a protoneutron star and its subsequent collapse to a black hole. We also study the neutrino signals that may be used as a probe to core collapse supernova. We adopt the newly constructed Shen hyperonic EoS for the simulation and compare the results with those of Shen nuclear EoS and understand the role of strange baryons in the core collapse.

1. Introduction

In recent years existence of strange matter in the high-density core of neutron stars has been the subject of extensive research [1–5]. It may so happen that the phase transition from hadronic to exotic phases might have already occurred in the early post-bounce phase of a core-collapse supernova. This idea of appearance of strange particles has initiated intense interest lately. It is said that a quark-hadron phase transition could trigger the explosion and revive the shock in supernova explosion, that was stalled due to loss of energy [6]. The neutrino burst ceases once the shock is stalled. However, an additional burst of neutrino is released if the shock revives. This could be a significant observational signature [6].

A supernova explosion usually leaves either a neutron star (NS) or a black hole (BH) as a remnant, depending on the initial conditions of the star. If the dense remnant is able to withstand the huge gravity, a protoneutron star (PNS) is formed, otherwise the star collapses into a black hole. The core collapse supernova explosion mechanism is being investigated over the last five decades. One of the main inputs in the study of evolution of core-collapse supernovae by numerical simulations, is the equation of state (EoS) for a wide range of density ($10^4 - 10^{15}$g/cm^3), temperature ($0 - 100$ MeV) and composition (proton fraction $0 - 0.6$) [7]. For the supernovae simulations with non-strange particles like neutrons (n), protons (p), alpha-particles (α) and nuclei, mainly two sets of EoS are used — Lattimer-Swesty (LS) [8] and Shen, Toki, Oyamatsu and Sumiyoshi (Shen) EoS [9]. The first EoS with non-nucleonic degrees of freedom was presented by Ishizuka et. al. [10]. They studied the emergence of the full baryon octet in the dynamical collapse of a massive static star to a black hole formation [11]. This EoS was recently utilised to study the behaviour of black hole formation and neutrino emission with hyperons and/or pions in Ref.[12]. Another set of EoS with hyperon degrees of freedom was constructed for supernova simulations [13] using the relativistic mean field model (RMF).

It is obvious that the inclusion of strange degrees of freedom softens the EoS. A stiffer EoS can sustain more mass against the collapse. A soft EoS on the other hand favors lower maximum masses compared to the stars having nucleonic degrees of freedom only. The recent measurement of the Shapiro delay in the radio pulsar PSR J1614-2230 which yielded a mass of $1.97 \pm 0.04 M_{solar}$, puts an important constraint on the neutron star mass and may rule out most of the soft EoS [14]. However, it is at present not possible to rule out any exotica with the $1.97M_{solar}$ observation as many model calculations including hyperons and/or quark matter could still be compatible with

*Electronic address: sarmistha.banik@saha.ac.in

it [13, 15, 16]. Many of these approaches are model dependent and can accommodate a NS as massive as two suns.

In this paper, we report the effect of hyperons on the black hole formation using the spherically-symmetric General relativistic hydrodynamic code, *GR1D* [17], designed to follow the evolution of stars beginning from the onset of core collapse. We adopt two sets of the Shen EoS–for nucleon (np) [9] and hyperon (npY) degrees of freedom [13]. We comment on the neutrino signal that might be observed as a result of phase transition from nucleonic to hyperonic matter.

The paper is arranged as follows. In Section 2, we briefly describe the EoS, we adopted for the simulations. Section 3 is devoted to the numerical simulation we used to study the core collapse till black hole formation. We discuss our results in Section 4 and finally we summarise in Section 5.

2. The equation of state (EoS)

We use the nuclear and hyperonic equation of state by Shen et. al for our simulations [9, 13]. Shen nuclear EoS is based on a relativistic mean field model at intermediate and high densities ($\rho > 10^{14.2}$ gm/cm^3). At low temperature (T$\leq$ 14 MeV), and $\rho < 10^{14.2} gm/cm^3$, Thomas Fermi approximation is used. The non-uniform matter at low temperature and density is modelled to consist of free nucleons, α particles and heavy nuclei whereas at extremely low density ($\rho < 10^{10}$ gm/cm^3)and finite temperature uniform nucleon gas of n, p, α particles is considered. Leptons are treated as uniform, non-interacting relativistic particles and their contributions are added separately. Minimisation of free energy is done both for non-uniform matter and uniform nucleon gas at low density. The calculation has been done in the RMF model with the TM1 parameter set [18], the parameters of the model are obtained by fitting the experimental data for binding energies and charge radii of heavy nuclei. With the TM1 parameter set, the nuclear matter saturation density is $0.145 fm^{-3}$, the binding energy per nucleon is 16.3 MeV, the symmetry energy is 36.9 MeV and the compressibility is 281 MeV [18]. The authors showed that their model agreed with the relativistic Brueckner Hartree Fock results reasonably well. Shen et. al. included the Λs in their EoS table [13]. For the parameters of Λ hyperons, they use the experimental mass value $M_\Lambda = 1115.7$ MeV. The coupling constant for hyperon-vector meson interaction is taken based on naive quark-model and that of hyperon-scalar meson interactions is determined by fitting experimental binding-energies data for single-Λ hypernuclei [22]. Λs appear when the threshold condition $\mu_n = \mu_\Lambda$ is satisfied, where μ_n and μ_Λ are the chemical potentials of the neutron and Λ respectively. Other hyperons, Ξ & Σ are excluded due to their relatively higher threshold and lack of experimental data.

3. The numerical simulations

We use the open source code *GR1D* [17] for the supernova simulations. *GR1D* is a spherically-symmetric, general-relativistic Eulerian hydrodynamics code for low and intermediate mass progenitors. It is designed to follow the evolution of stars beginning from the onset of core collapse to black hole formation and makes use of several microphysical EoS.The metric of *GR1D* is given by the line element

$$ds^2 = -\alpha(r,t)^2 dt^2 + X(r,t)^2 dr^2 + r^2 d\Omega^2 \ ,$$

where $\alpha(r,t) = exp^{(\Phi(r,t))}$ with $\Phi(r,t)$ being a metric potential. $X(r,t) = [1 - 2m(r)/r]^{-1/2}$, m(r) is the enclosed gravitational mass. The stress-energy of an ideal fluid is given by

$$T^{\mu\nu} = \rho h u^\mu u^\nu + g^{\mu\nu} P. \qquad (1)$$

where ρ is the matter density, P is the fluid pressure and $h = 1 + \epsilon + P/\rho$ is the specific enthalpy, ϵ the internal energy. u^μ is the 4-velocity of the fluid and without rotation taken to be $(W/\alpha, Wv^r, 0, 0)$, where $W = [1 - v^2]^{-1/2}$ is the Lorentz factor and $v = Xv^r$ is the physical velocity. For a given matter configuration, the differential equation for $m(r)$ and $\Phi(r)$ are obtained from Hamiltonian and momentum constraint equations and

are

$$m(r) = 4\pi \int_0^r (\rho h W^2 - P + \tau_m^\nu) r'^2 dr' \quad (2)$$

$$\Phi(r,t) = \int_0^r X^2 Z dr' + \Phi_0 \ . \quad (3)$$

where $Z = \left[\frac{m(r',t)}{r'^2} + 4\pi r'(\rho h W^2 v^2 + P + \tau_m^\nu)\right]$. Here Φ_0 is determined by matching the metric at the star's surface to the Schwarzschild metric and τ_m^ν accounts for the trapped neutrinos. The evolution equations for the matter fields are derived from the local conservation laws $\nabla_\mu T^{\mu\nu} = 0$ and $\nabla_\mu J^\mu = 0$, and are given by

$$\partial_t \vec{U} + \frac{1}{r^2}\partial_r \left[\frac{\alpha r^2}{X}\vec{F}\right] = \vec{S} \quad (4)$$

where $\vec{U}$ is the set of conserved variables, $\vec{F}$ is their flux vector, and $\vec{S}$ is the vector containing gravitational, geometric and neutrino-matter interaction sources and sinks, which arise from the neutrino leakage scheme [17].

Neutrino effects are crucial in stellar collapse, they are the source of both cooling as well as heating. Neutrino emission takes place when electrons are captured by free or bound protons leading to fall of lepton number Y_e at the core ($e^- + p \longrightarrow \nu_e + p$). Neutrino emission should ideally be included via a computationally expensive GR Boltzmann transport treatment (such as Liebendörfer et. al. [19]). However, since the aim is an extensive parameter study with hundreds of simulations, a less accurate, but much computationally efficient leakage and approximate heating scheme for neutrinos are chosen in this code. Before core bounce, neutrino deleptonisation reduces the size of the inner core. Y_e is parameterized as a function of density according to Liebendörfer's prescription [19]. However, post bounce it can not capture the effect of neutrino cooling, deleptonisation and neutrino heating. Hence a 3-flavor, energy-averaged neutrino leakage scheme ($Q^- \propto T^{-6}$, where T= temperature) is adopted. This captures the effects of cooling. Here three neutrino species– $\nu_e, \bar{\nu}_e, \nu_\mu, \bar{\nu}_\mu, \nu_\tau, \bar{\nu}_\tau$ are considered. The leakage scheme provides approximate energy and number emission rates and are included into $GR1D$'s evolution equations through source terms $\vec{S}$. Neutrino heating ($\nu_e + n \longrightarrow e^- + p$, $\bar{\nu}_e + p \longrightarrow e^+ + n$) is included via a parameterized charged-current heating scheme ($Q_\nu^+ \propto L_\nu r^{-2} < \epsilon_\nu^2 >$, where $L_\nu, < \epsilon_\nu^2 >$ are the luminosity and averaged energy density of neutrino at some radius r) based on Ref. [20].

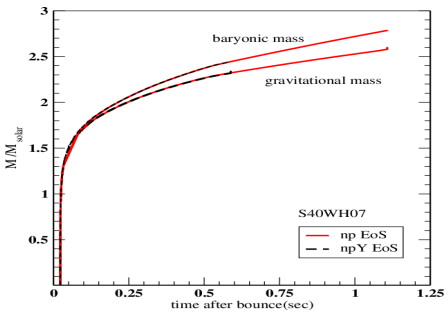

FIG. 1: Baryonic mass and gravitational mass vs. time after bounce for the s40WW07 progenitor with Shen np and npY EoS

4. Results & Discussion

We report our simulation results for a $40 M_{solar}$ progenitor model of Woosley et. al [21] using GR1D [17] for Shen EoS- nucleon (np) as well as and hyperon (npY) [9, 13]. We solved the Tolman-Oppenheimer-Volkov equation for zero temperature (T=0) EoS of NS assuming β equilibrium. The maximum mass of the NS for np EoS is 2.18 M_{solar}, whereas for npY EoS, the maximum mass reduces to $1.82 M_{solar}$. The corresponding radii are 12 and 12.5 km respectively.

In Fig. 1 we plot the baryonic and gravitational mass of PNS, obtained from simulations. The maximum mass is higher than that of NS. When accretion pushes PNS over its maximum mass, BH is formed. The spikes in the gravitational mass correspond to a blow-up and the BH formation. For the np EoS, this happens for a $2.71 M_{solar}$ star at 1.09 s after bounce, whereas for npY EoS (the black dashed lines) this happens much earlier at 0.57

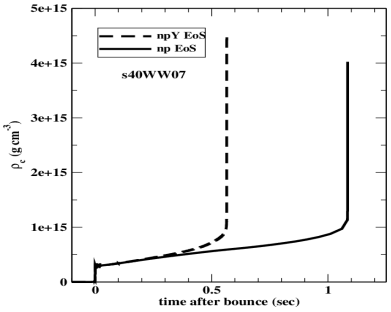

FIG. 2: Central density (ρ_c) vs time after bounce for the s40WW07 progenitor with Shen np and npY EoS

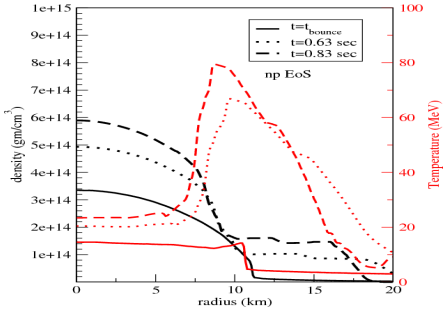

FIG. 4: Density and temperature profiles vs radius for np EoS

s after bounce for a $2.38 M_{solar}$ star.

Fig. 2 shows the evolution of central density (ρ_c) for the np (solid lines) and npY EoS (dashed lines). The bounce corresponds to the spikes at real timeline $t_{bounce} = 0.27$ s, which we take as t=0 in the figure. The value of t_{bounce} is same for the np and npY EoS, we will see that the contribution of hyperon is not important at that time. The onset of BH formation is marked by a sharp rise in the value of ρ_c. Similar trend is noticed in the temperature profile. Owing to the hyperon emergence, the contraction of PNS is accelerated, which leads to quicker rise in temperature and central density. Or in other words, the stiffer EoS leads to larger post-bounce time to BH-formation.

It is of particular interest to see when hyperons appears first in the collapse. We display the evolution of mass fraction of neutrons and Λs with time for a proton fraction of 0.28 in Fig. 3. Initially at core bounce the system consists of neutron and protons only; Λs appear at 0.16 s after core bounce (assuming 10^{-3} considerable amount of fraction). The appearance of Λ hyperon is delayed until the matter density reaches at least $2\rho_0(\rho_0 \simeq 2.410^{14}\ gm/cm^3)$, the threshold shifts to lower density with increasing temperature [13]. We have seen the central density at bounce is just above normal nuclear matter density (Fig 2). The central density and temperature increase with time at the core of the star and at 0.16 s after bounce rise to $3.79x10^{14}\ gm/cm^3$ and 16.26 MeV respectively. The Λs may be formed at the cost of the nucleons through $n + p \longrightarrow p + \Lambda + K^0$, so neutron population goes down as soon as they appear.

In Figs. 4 and 5, we compare the density

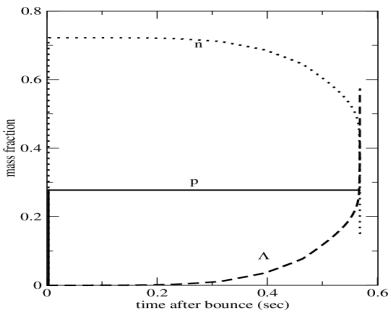

FIG. 3: Evolution of particle fraction for the s40WW07 progenitor

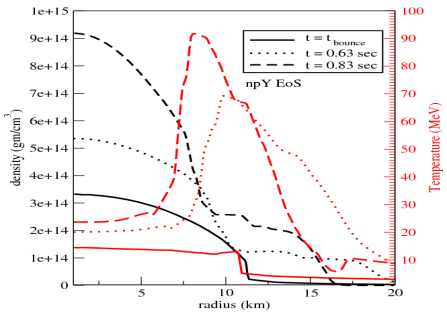

FIG. 5: Density and temperature profiles vs radius for npY EoS

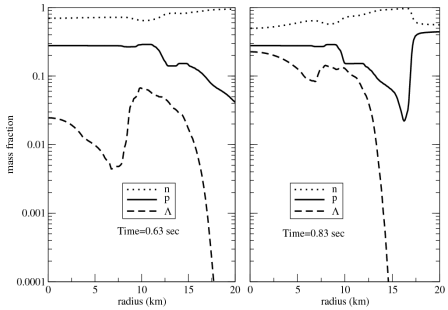

FIG. 6: Snapshot of particle fraction vs. radius at t=0.63 s and 0.83 s

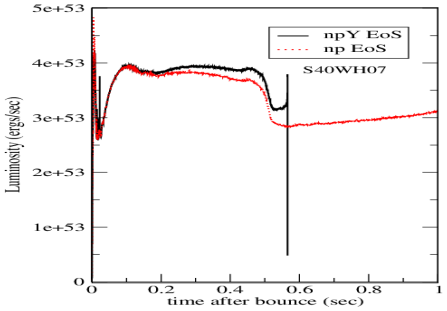

FIG. 7: Luminosity of total neutrinos as a function of time after bounce.

(black lines) and temperature (red lines) profiles for np and npY cases at t=t_{bounce}, 0.63 s and 0.83 s. The density and temperature profiles are similar in both the cases. The density rises from less than ρ_0 at the surface to a few times ρ_0 at the core. The plateau in the density profile could be attributed to strong thermal pressure there. At core bounce, the core density is $1.4\rho_0$. With intense accretion, the central density shoots to $2\rho_0$ at 0.63 s, and $2.5\rho_0$ at 0.83 s for np EoS. The central density is slightly above that of the np case at t=0.63 s, as Λ just starts appearing in the system. However, as evident from Fig. 3, at t=0.83 s, there is substantial amount of Λ in the system and the central density rises almost $3.8\rho_0$, which is 2.8 times its value at core bounce.

With time, the temperature also attains a peak at the mid-radius region. The peak rises from 66.8 Mev at 0.63 s to 79.35 Mev at 0.83 s in np case (Fig. 4). This is due to accretion and compression of shock heated material onto the PNS surface. At this region, the thermal pressure support is enough to flatten the density profile. In inner core ($\sim$ 6km) the material is not shock heated, rather is heated by adiabatic compression. The temperature peak is further raised to 91.7 MeV at 0.83 s in the presence of Λ hyperons (Fig. 5).

Next we compare the compositions of PNS in Fig. 6. Two snapshots at 0.63 s and 0.83 s after core bounce are displayed in the two panels. It is interesting to note that hyperons appear off-center owing to high temperature, although density is still on the plateau (Fig. 5). At 0.63 s after core bounce, the abundance of Λ becomes significant at R $\simeq$ 10km, as temperature is maximum there (Fig. 5). It even falls sharply after reaching the peak due to fall in temperature, only to rise at the core again owing to high density there. At a later time, the high central density forbids it from dropping too low, once it reaches the peak at mid-radius region. Thus, Λ becomes one of the major components at the core.

In the final figure, the evolution of neutrino-luminosity is plotted for the np and npY EoS. We find a short neutrino burst ($\sim$ 1s) before the PNS, born temporarily in a failed-supernova, terminates in a black hole. The resulting neutrino burst in np and npY cases are quite similar, differ only in earlier termination of burst in the latter. The soft npY EoS lowers the critical mass of PNS, thus accelerates the mass accretion onto it and triggers the gravitational instability at 0.63 s. However, no second neutrino burst is noticed as observed in quark-hadron phase transition [6]. The quark EoS is stiff while the npY is a soft one. So, npY though triggers black hole formation, fails to generate second shock.

5. Summary

We have studied the effect of hadron-hyperon phase transition in core-collapse supernova using general relativistic hydrodynamic simulation GR1D [17]. By following the dynamical collapse of a new-born proto-neutron star from the gravitational collapse of a $40M_{solar}$ star adopting Shen hyperonic EoS

table[13], we notice that hyperons appear just before bounce. It appears off center at first due to high temperature and prevails at the center just before the black hole formation, when the density becomes quite high. Hyperons triggers the black-hole formation, but fails to generate the second shock as the EoS is softened too much with the appearance of hyperons. Hyperon emergence in the collapse produces an intense but short neutrino burst, which terminates at the black hole formation. However, no second neutrino burst is observed as in quark-hadron phase transition.

There are possibilities for other strange degrees of freedom in the form of kaon condensates to appear in the highly dense matter. We have seen such a phase transition can support a maximum mass [2], which is well above $2M_{solar}$ [14]. It would be intriguing to investigate if a hadron-antikaon condensed matter can revive the second shock. A successful shock revival would have observational consequence in the form of neutrino signatures. Post SN1987A, advanced neutrino facilities such as Ice-cube and Super-kamiokande should detect the neutrino signals [23].

Acknowledgments

The author thanks Debades Bandyopadhyay, Evan O'connor and Christian Ott for stimulating discussions.

References

[1] N.K. Glendenning, Compact stars, (Springer, New York, 1997).
[2] S. Banik and D. Bandyopadhyay, Phys. Rev. **C63** 035802 (2001).
[3] S. Banik and D. Bandyopadhyay, Phys. Rev. **C64** 055805 (2001).
[4] S. Banik and D. Bandyopadhyay, Phys. Rev. **C66** 065801 (2002).
[5] S. Banik and D. Bandyopadhyay,Phys. Rev. **D67** 123003 (2003).
[6] T. Fischer, I. Sagert, G. Pagliara, M. Hempel, J. Schaffner-Bielich, T. Rauscher, F.K. Thielemann, R. Kppeli, G. Martnez-Pinedo, M. Liebendrfer ApJ. Supp. **194** 39, (2011).
[7] M. Hempel and J. Schaffner-Bielich, Nucl. Phys. A **837** 210 (2010).
[8] J. M. Lattimer and F. D. Swesty, Nucl. Phys. A **535** 331 (1991).
[9] H. Shen, H. Toki, K. Oyamatsu, K. Sumiyoshi, Nucl.Phys. **A637** 435 (1998).
[10] C. Ishizuka, A. Ohnishi, K. Tsubakihara, K. Sumiyoshi, S.Yamada, J. Phys. **G35** 085201 (2008).
[11] K. Sumiyoshi, C. Ishizuka, A. Ohnishi, S. Yamada, H. Suzuki, APjL, **690**, L43 (2009).
[12] K. Nakazato, S. Furusawa, K. Sumiyoshi, A. Ohnishi, S. Yamada, H. Suzuki, Astrophys.J.**745** 197 (2012).
[13] H. Shen, H. Toki, K. Oyamatsu, K. Sumiyoshi, ApjS, **197**, 20 (2011).
[14] P. B. Demorest, T. Pennucci,S. M. Ransom, M. S. E. Roberts & J. W. T. Hessels, Nature **467** 1081 (2010).
[15] J. M. Lattimer, M. Prakash, arXiv:1012.3208
[16] E. Massot, J. Margueron, and G. Chanfray, EPL **97** 39002 (2012)
[17] E. O'Connor, C. D. Ott, ApJ **730** 70 (2011)
[18] Y. Sugahara and H. Toki, Nucl. Phys. **A579** 557 (1994).
[19] Matthias Liebendörfer, Astrophys.J. **633** 1042 (2005)
[20] H.Th. Janka, A & A, **368**, 527 (2001)
[21] S. E. Woosley, A. Heger, and T. A. Weaver, Rev. Mod. Phys. **74** 1015 (2002).
[22] H. Shen,F. Yang, H. Toki, Prog. Theo. Phys., **115** 325 (2006).
[23] B. Dasgupta, A. Mirizzi, I. Tamborra, R. Tomas, Phys. Rev. **D81** 073004 (2010).